Ultrafast magnetization dynamics:
from continuous films to nanoparticles

Mark Freeman
with Miro Belov, Kristen Buchanan, BC Choi, Grey Arnup, Sasha Krichevsky, Zhigang Liu, Al Meldrum, Xiaobin Zhu

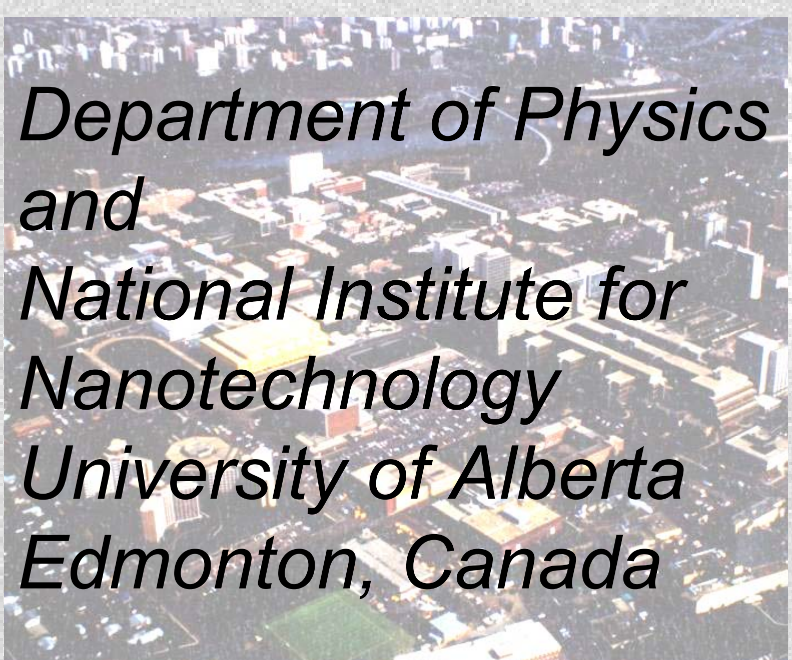

Department of Physics
and
National Institute for Nanotechnology
University of Alberta
Edmonton, Canada

Supported by
NSERC
iCORE
CIAR
CRC

motivation: study the influence of structure on magnetization dynamics
approach: time-domain, local probing, including stroboscopic imaging and “ripple tank” experiments with magnetic oscillations in mesoscopic ferromagnets
theme for the workshop: opportunities created by the ability to attack these problems with x-rays

- major gains: spatial resolution (including ability to image static configurations with high resolution, important as initial conditions for dynamics); chemical selectivity;
- neutral: temporal resolution
- sacrifices: capability for vector measurement; ability to probe stochastic phenomena, potential for single-shot imaging

outline

• mode control in lithographic elements: small angle precession

• large angle excitation during switching:

-- oscillations and damping

• nanocrystalline composites:

-- exchange and dipolar vs. only dipolar coupling between “giant classical spins”

• comparison of experiment and numerical modeling

•discussion and prospects

Magnetic Structures

Magnetic domain structure is a function of the geometry:

Xiaobin Zhu,
MFM

patterned film

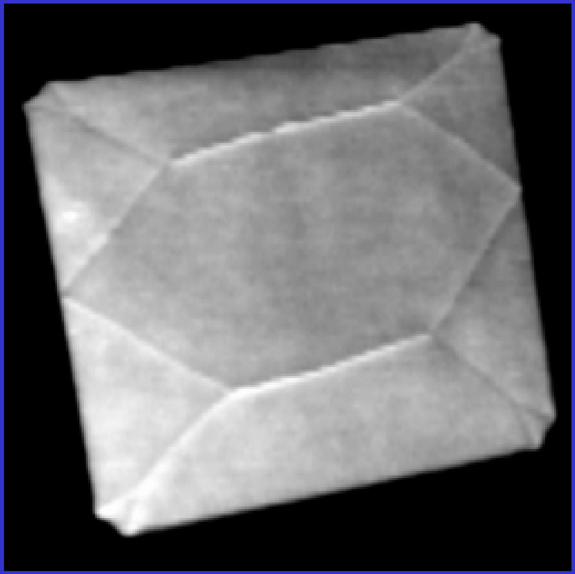

25 μm x 25 μm

20 μm permalloy square

single domain

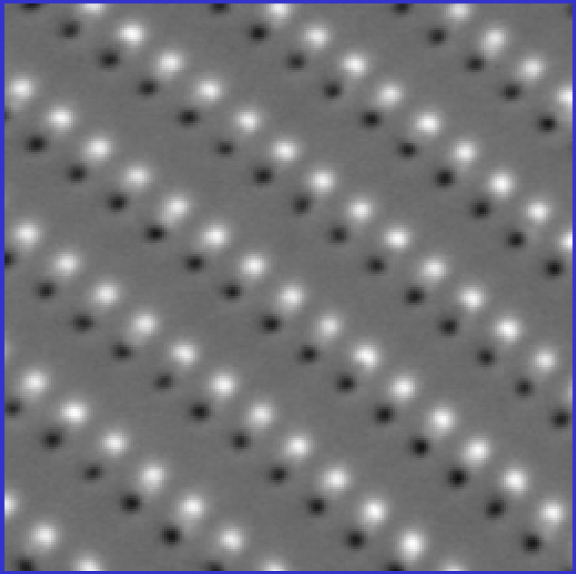

3 μm x 3 μm

Particle size:
240 nm x 90 nm x 10nm

Spin Dynamics

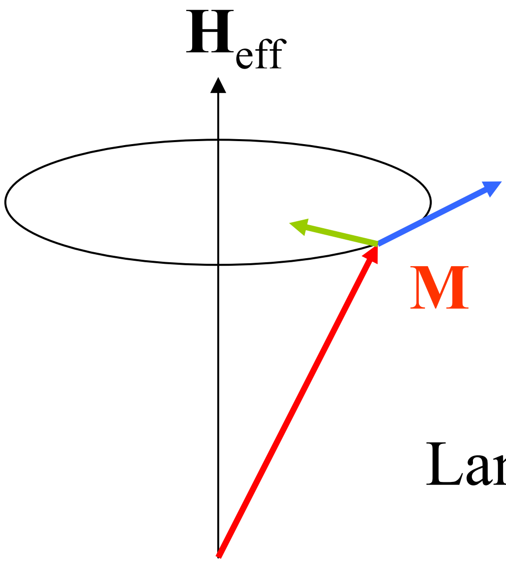

$$\frac{\partial M}{\partial t} = \gamma[M \times H_{eff}] - \alpha\gamma[M \times M \times H_{eff}]$$

Landau-Lifshitz-Gilbert Equation

α: 0.002 (Fe) 0.011 (Co)

0.019 (Ni) 0.006 (NiFe)

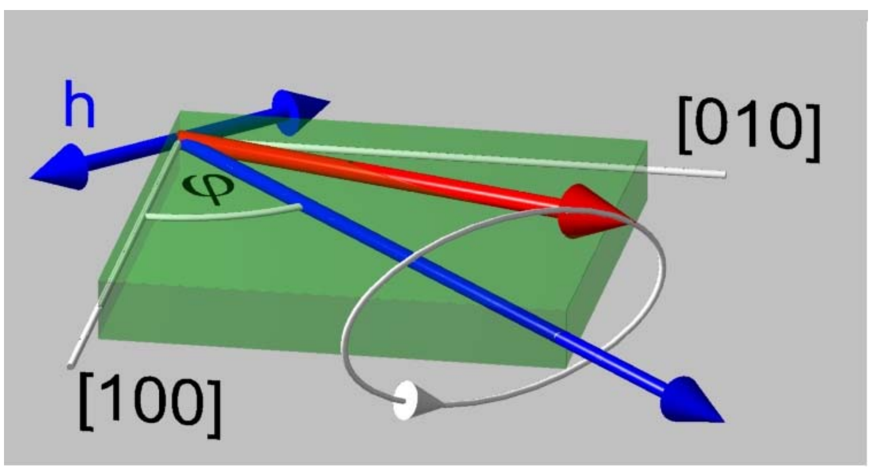

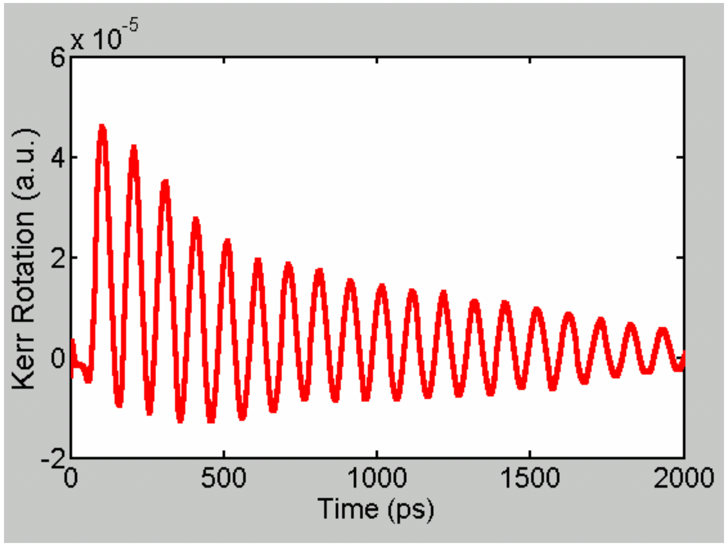

Large Angle Precession, Switching

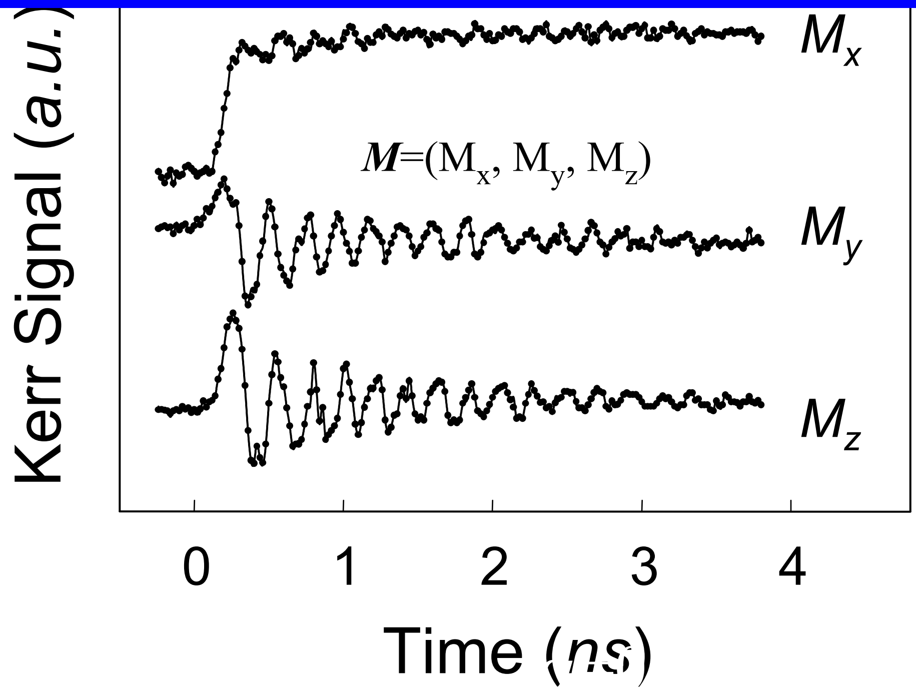

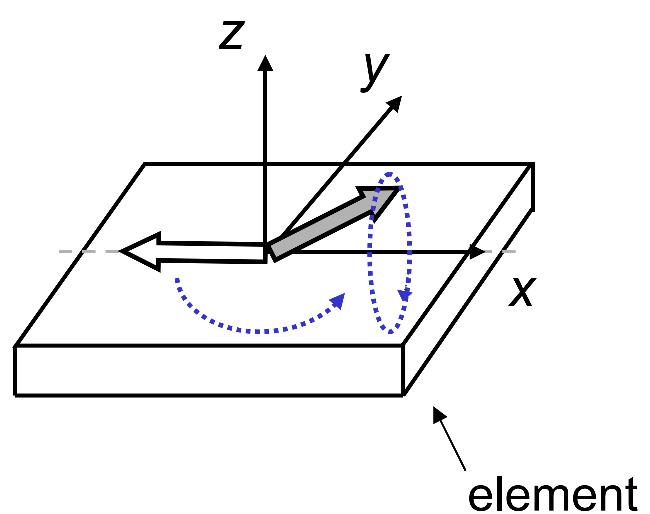

Oscillation after ‘switching’

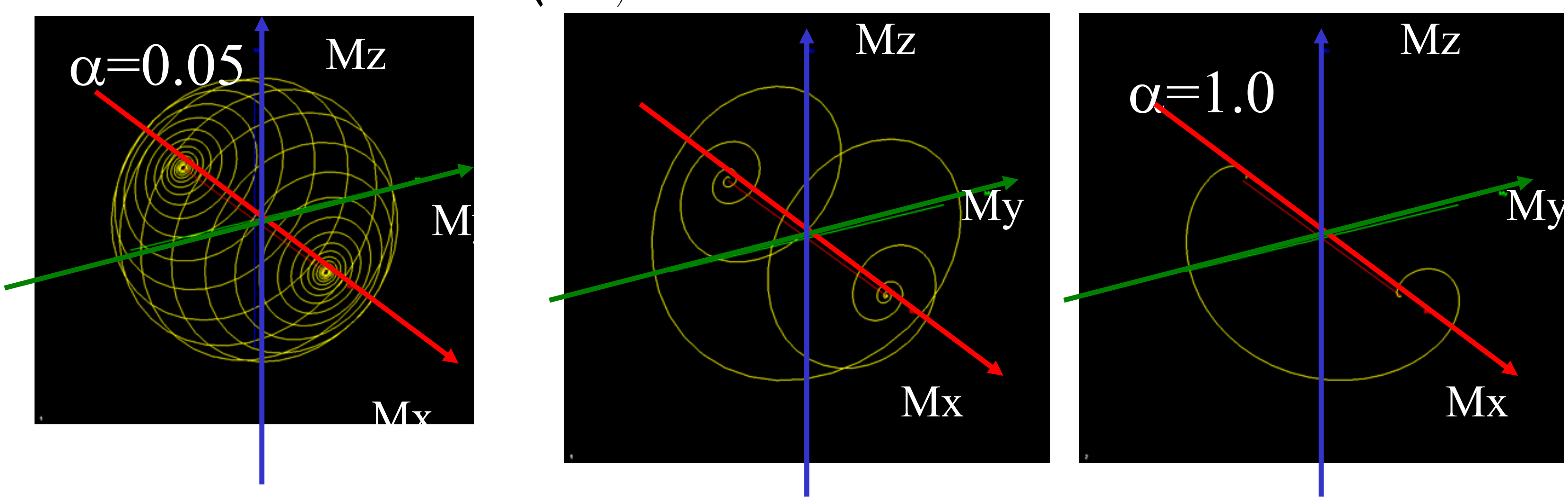

time-resolved scanning Kerr microscopy

high bandwidth from short optical pulses; high-speed information from relative timing

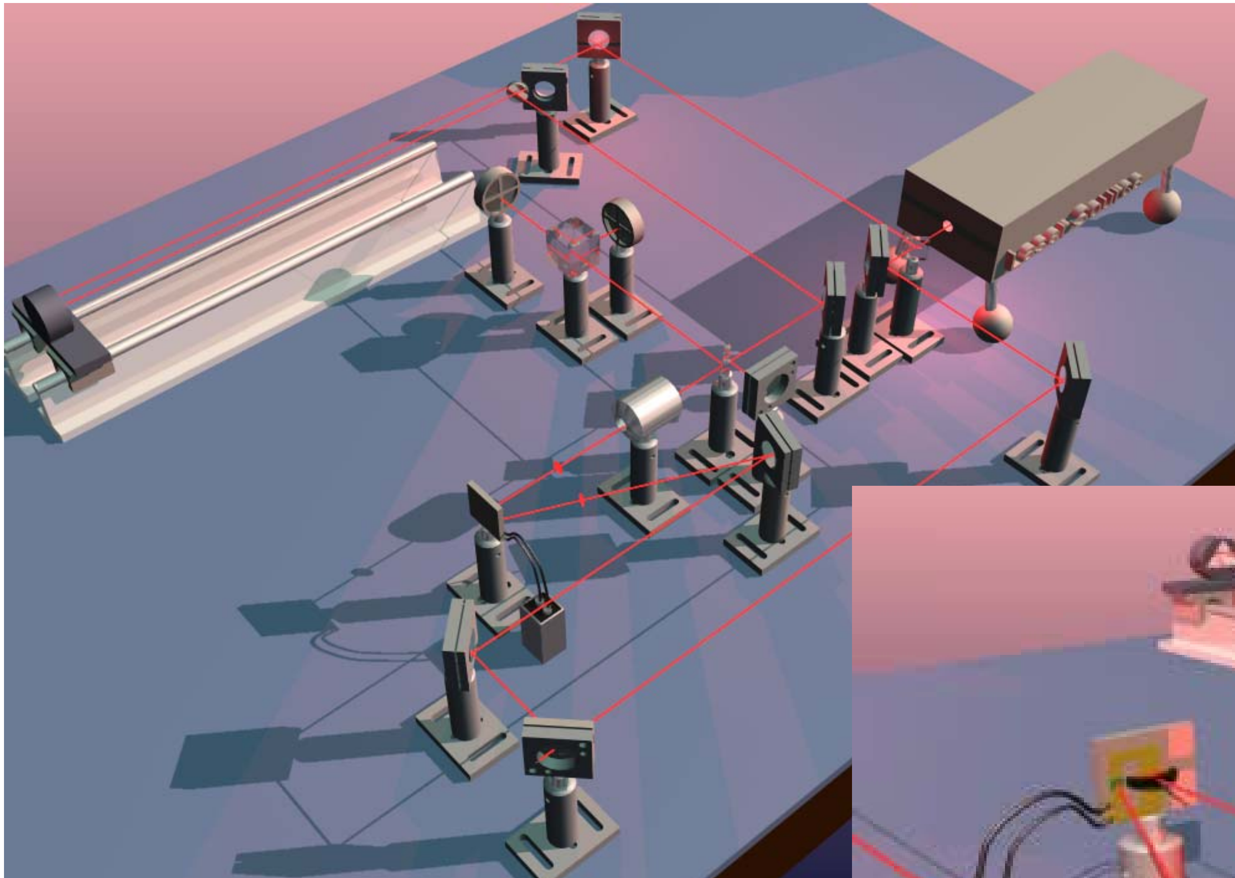

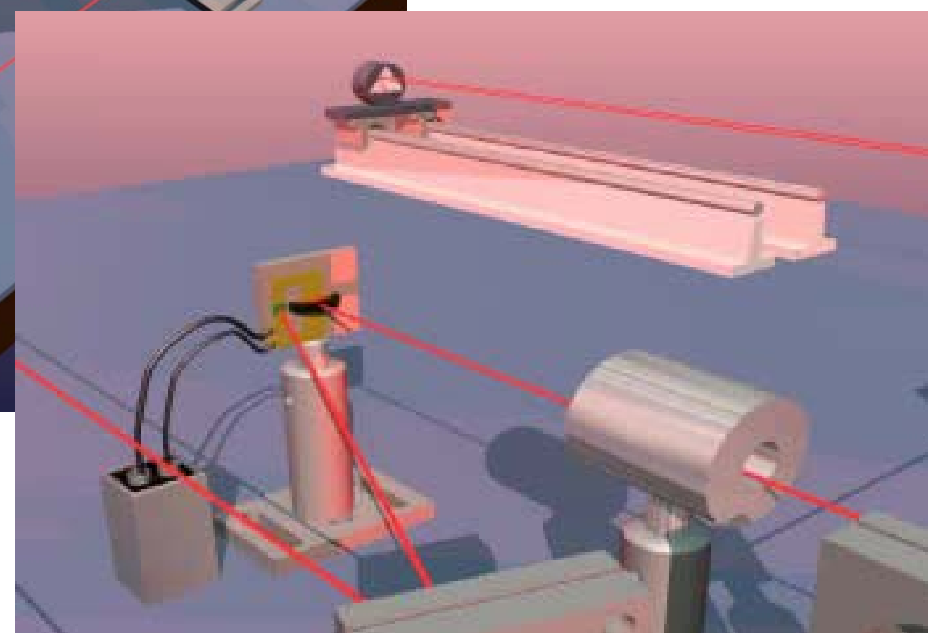

Dave Fortin

http://nanoscale.phys.ualberta.ca

time-resolved scanning Kerr microscopy

specimen geometry for both in- and out-of-plane transient excitation

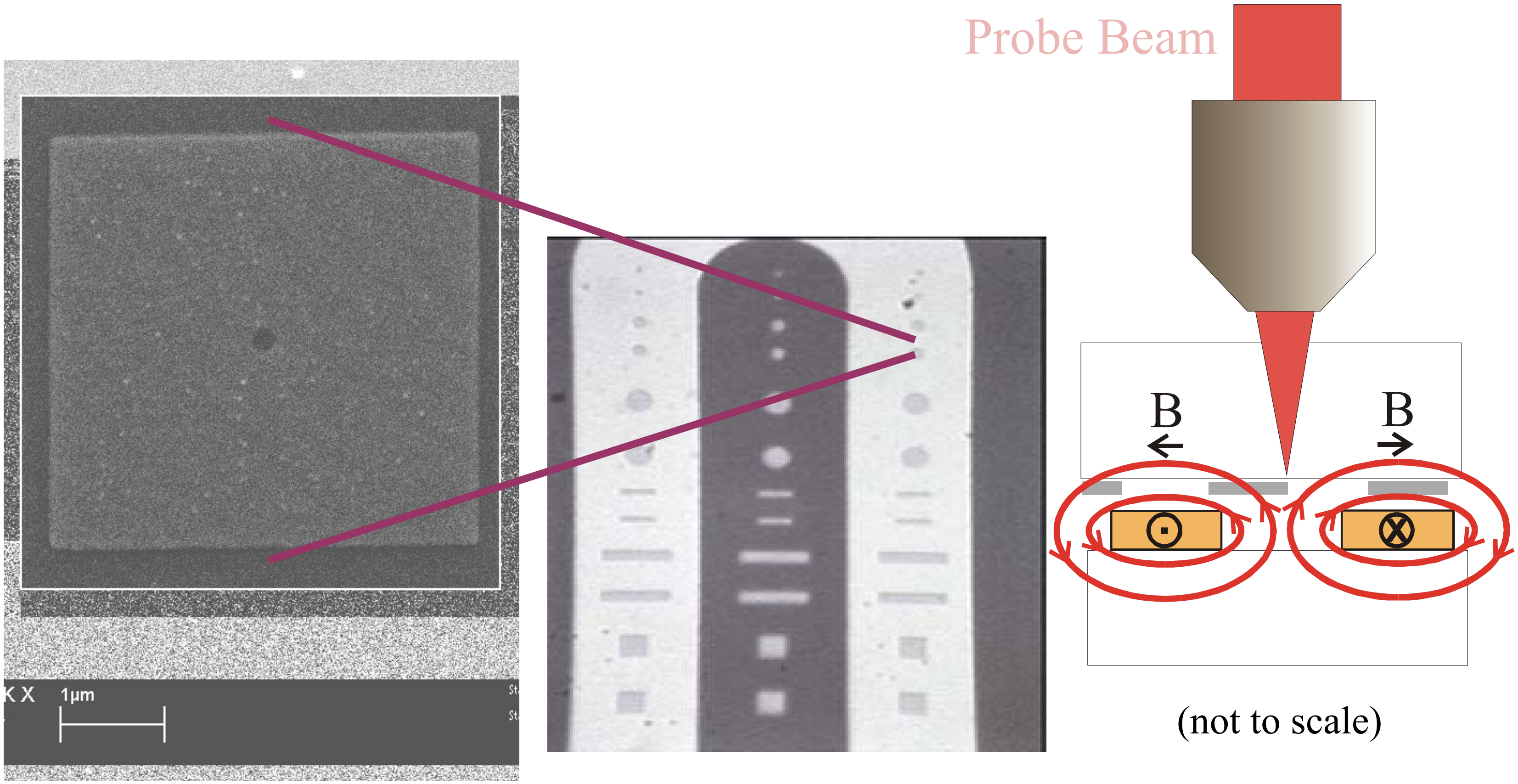

- “pump” provides fast transient magnetic field (current pulse traveling through transmission line)

Miro Belov

"vector magnetometer": quadrant detection scheme

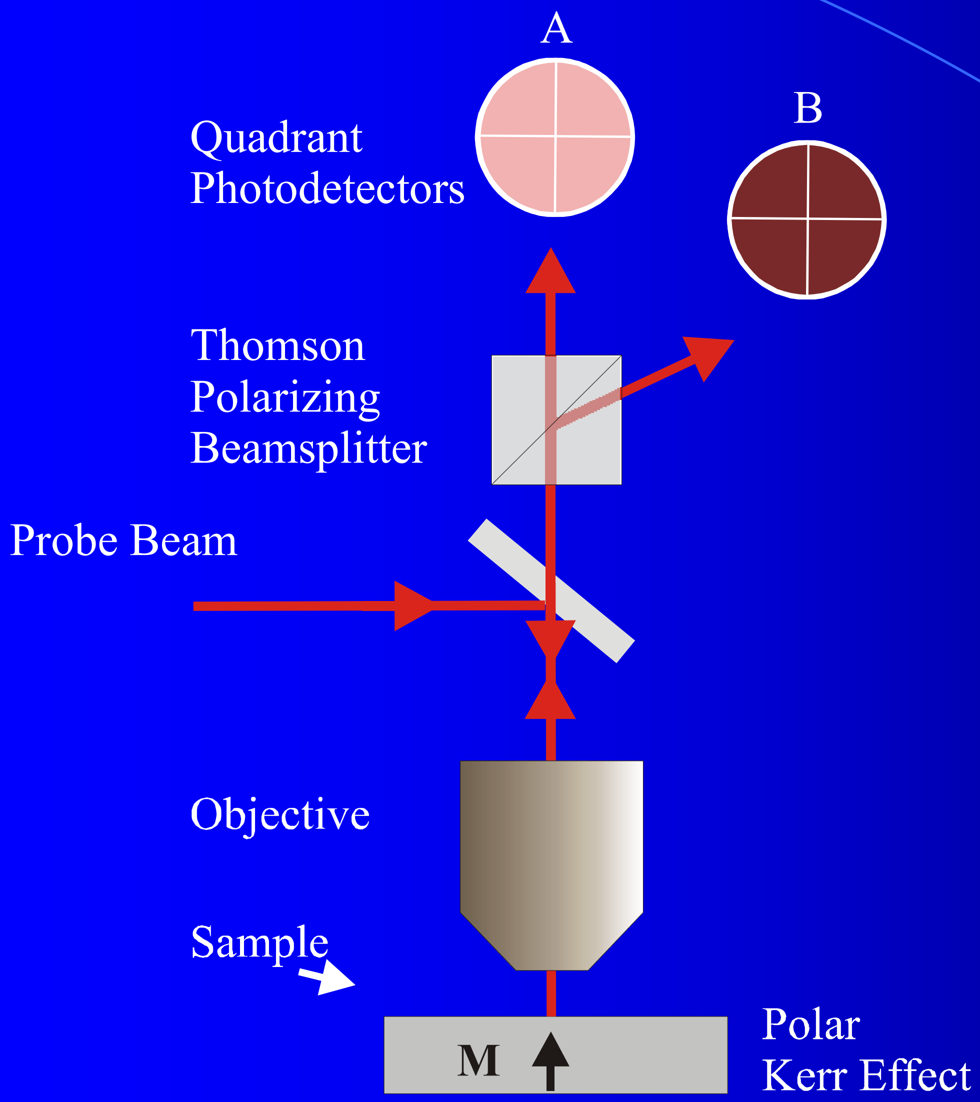

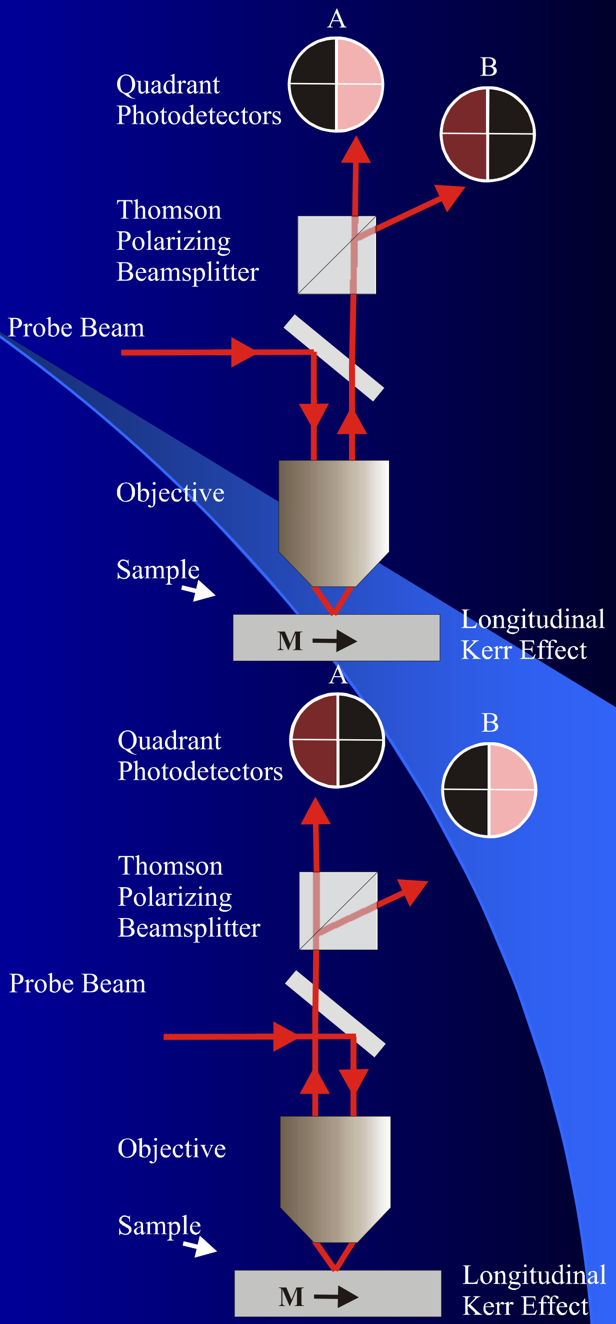

A. Krichevsky,
K. Buchanan

polar

longitudinal

FMR response to transient out-of-plane field

small tipping angle, 51 Oe DC bias field

polar Kerr signal:

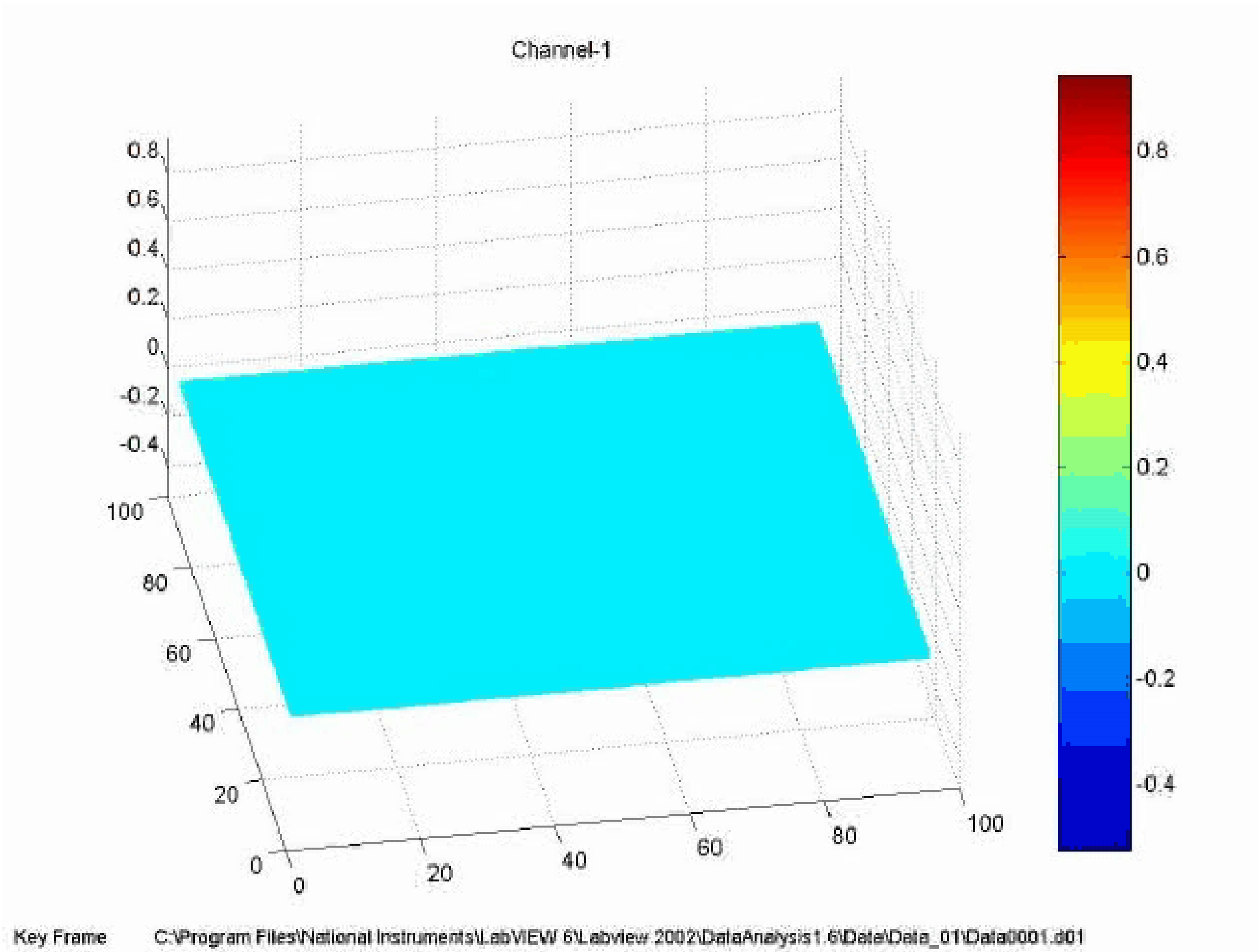

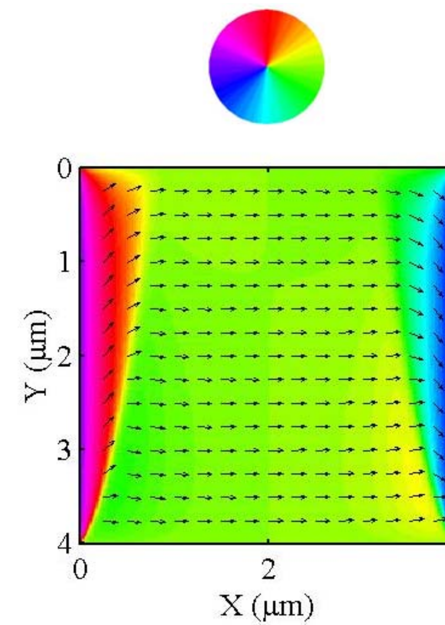

initial C state
(from simulation)

H_{bias} → $H_{transient}$ ⊙

M. Belov

"snapshots" of out-of-plane magnetization, square specimen with and without pinhole

4.6 kA/m in-plane bias

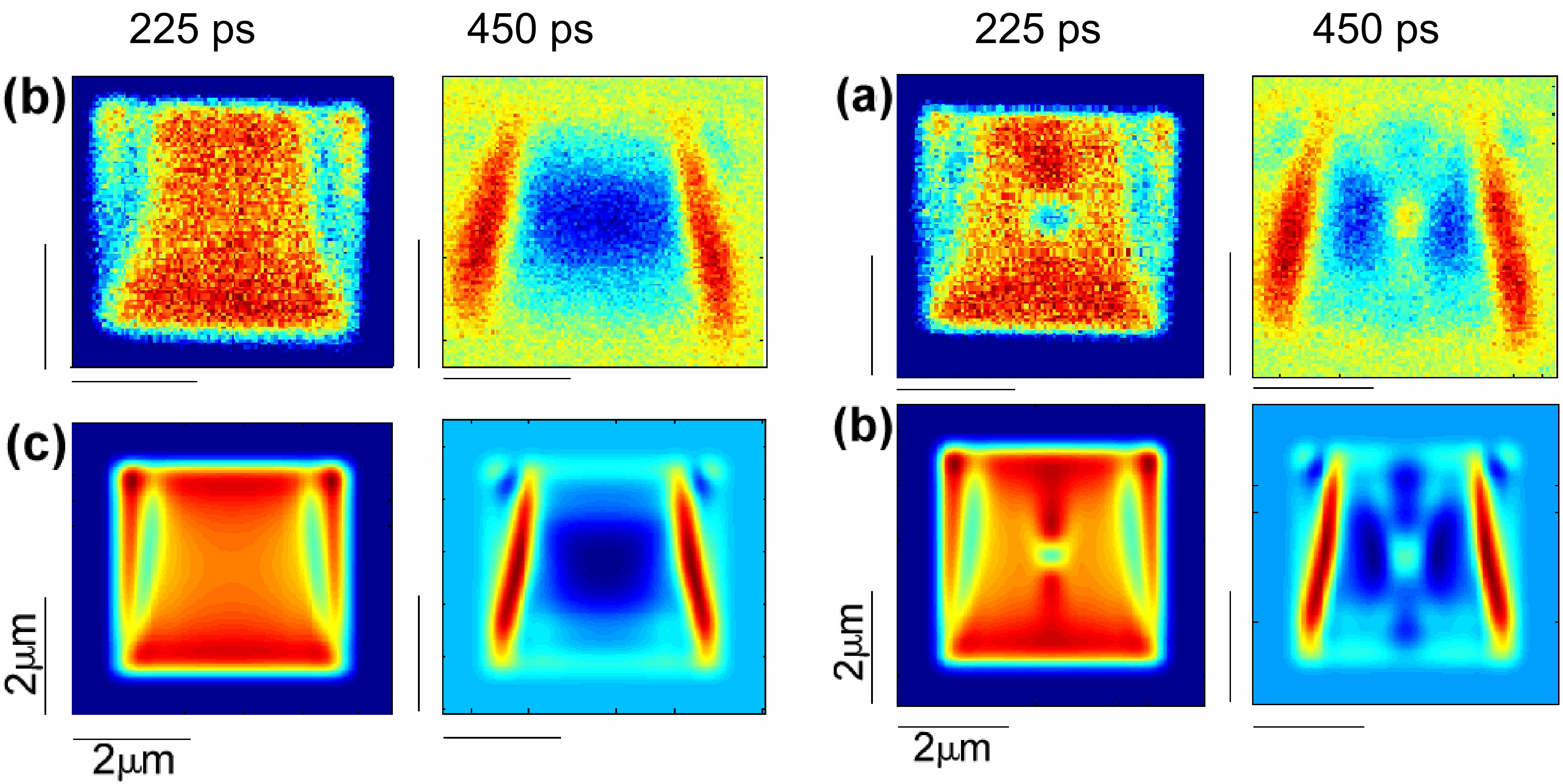

modal oscillations conform to symmetry of nonuniform magnetization

M. Belov *et al.,* PRB **69** (2004): 94414

position-dependent effective damping

as revealed in “x vs. t” cross sections

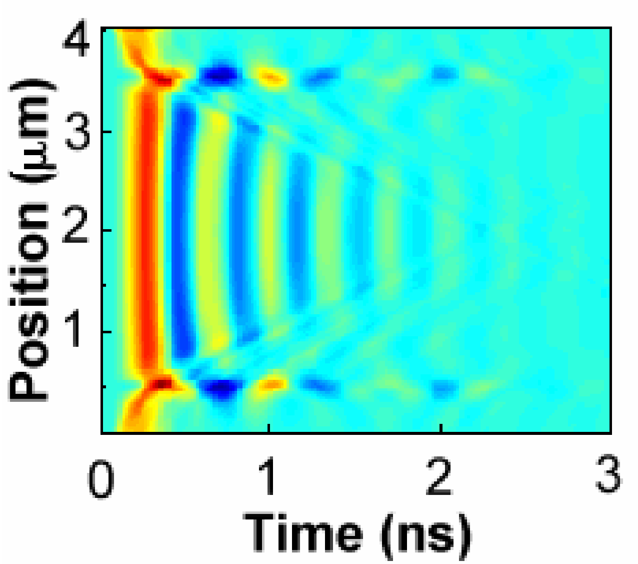

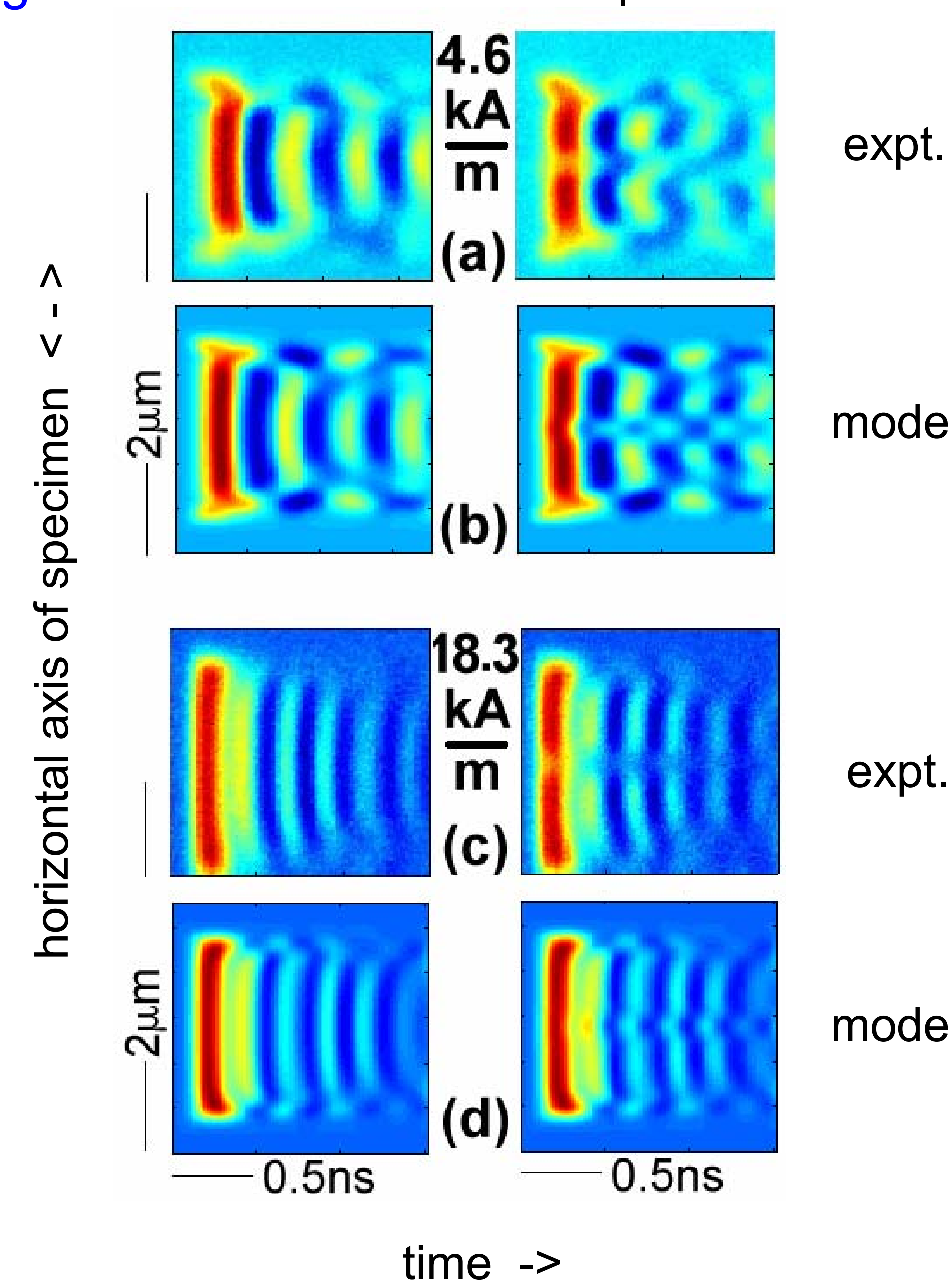

M. Belov

large amplitude excitation of low frequency closure domain mode

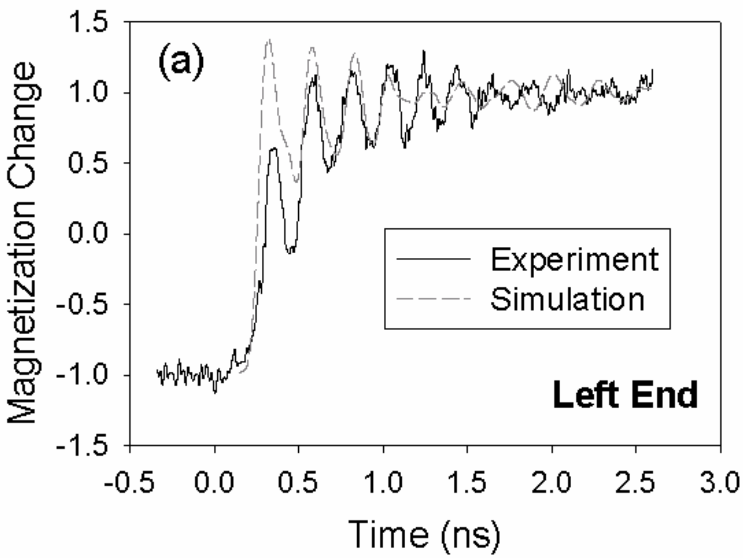

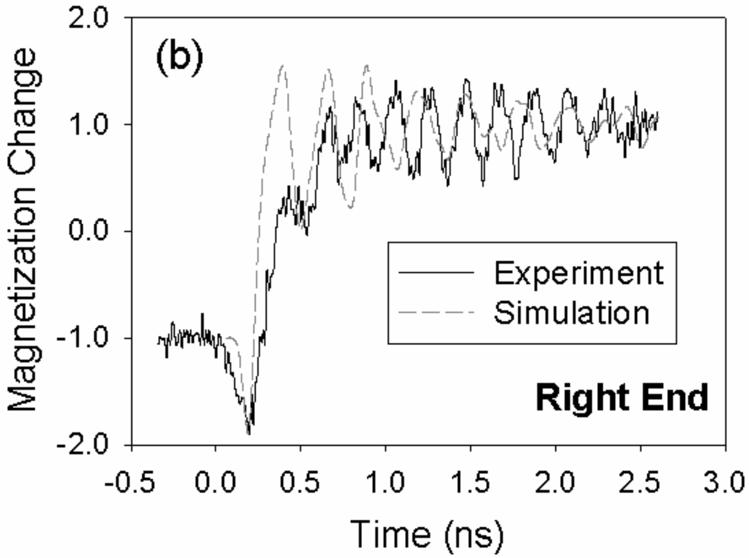

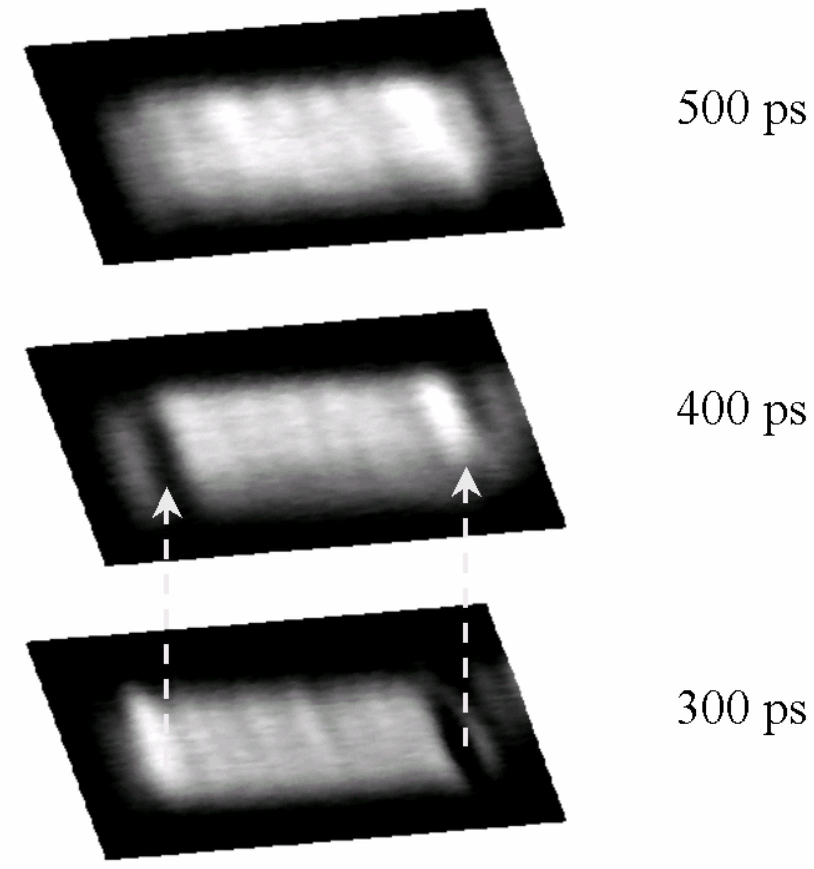

- this measurement is an admixture of the longitudinal (easy-axis) and polar components
- perhaps stronger suppression of initial out-of-plane excursion in expt.

relative to sim. owing to sample imperfections; finite spatial resolution of msmt.

transient closure domains also exhibit large amplitude oscillations

form at long sides owing to dipolar interaction resisting switching of the edges

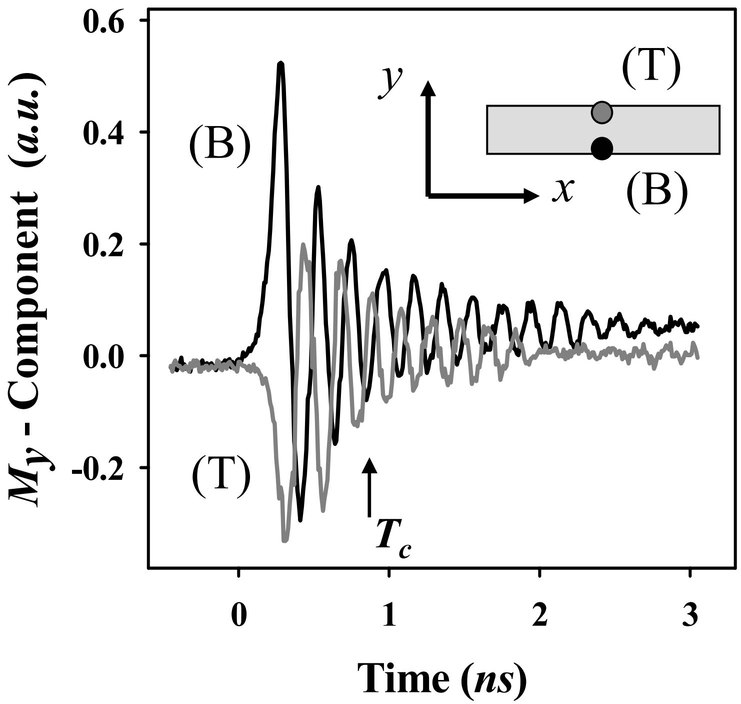

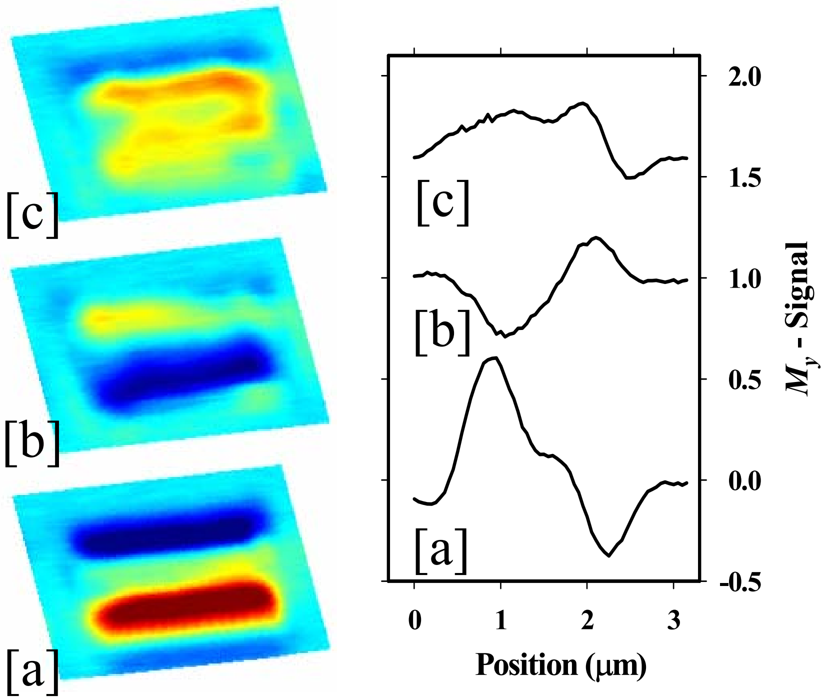

time-resolved images of in-plane hard-axis magnetization component, with line cuts

B.C. Choi *et al.*, JAP **95** (2004): 6540 envelope of the decay:

accelerated early ringdown, owing to energy transfer to short wavelength modes; reasonably accounted for by finite-element LLG

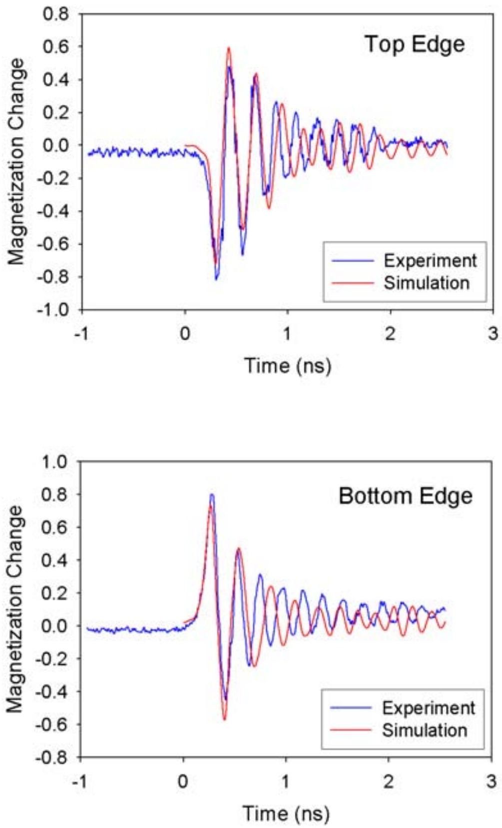

comparison to simulation:
finite element LLG with α = 0.01

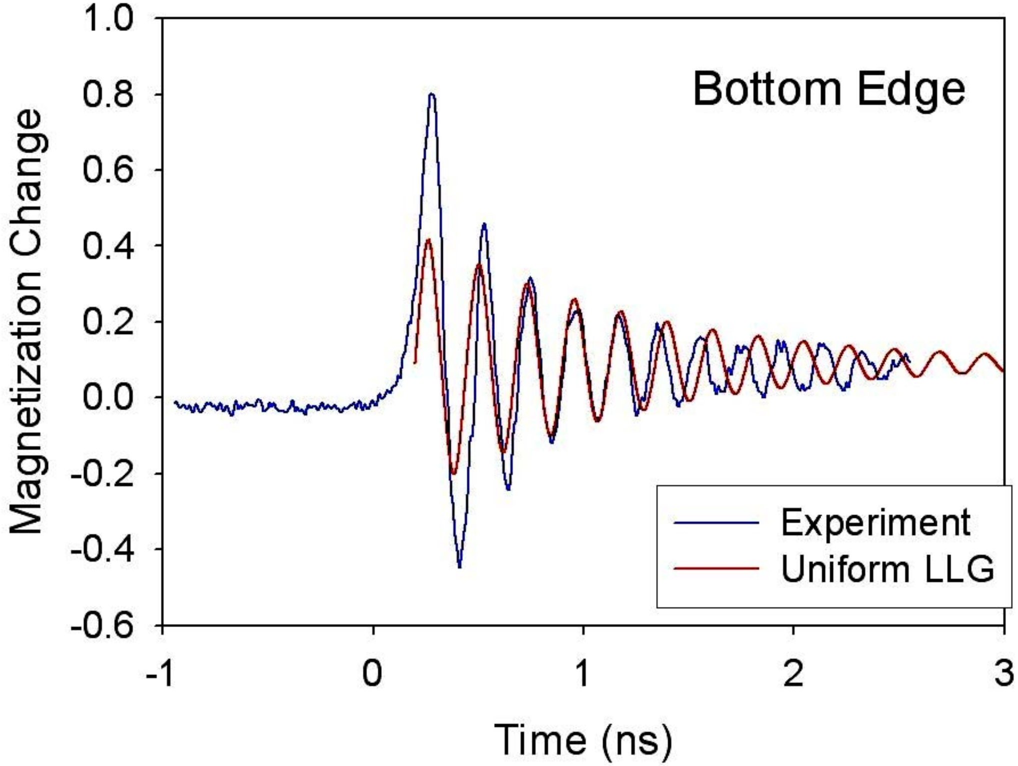

comparison to simulation:
uniform LLG with α = 0.01

switching with simultaneously acting easy- and hard-axis pulses

in typical MRAM geometry

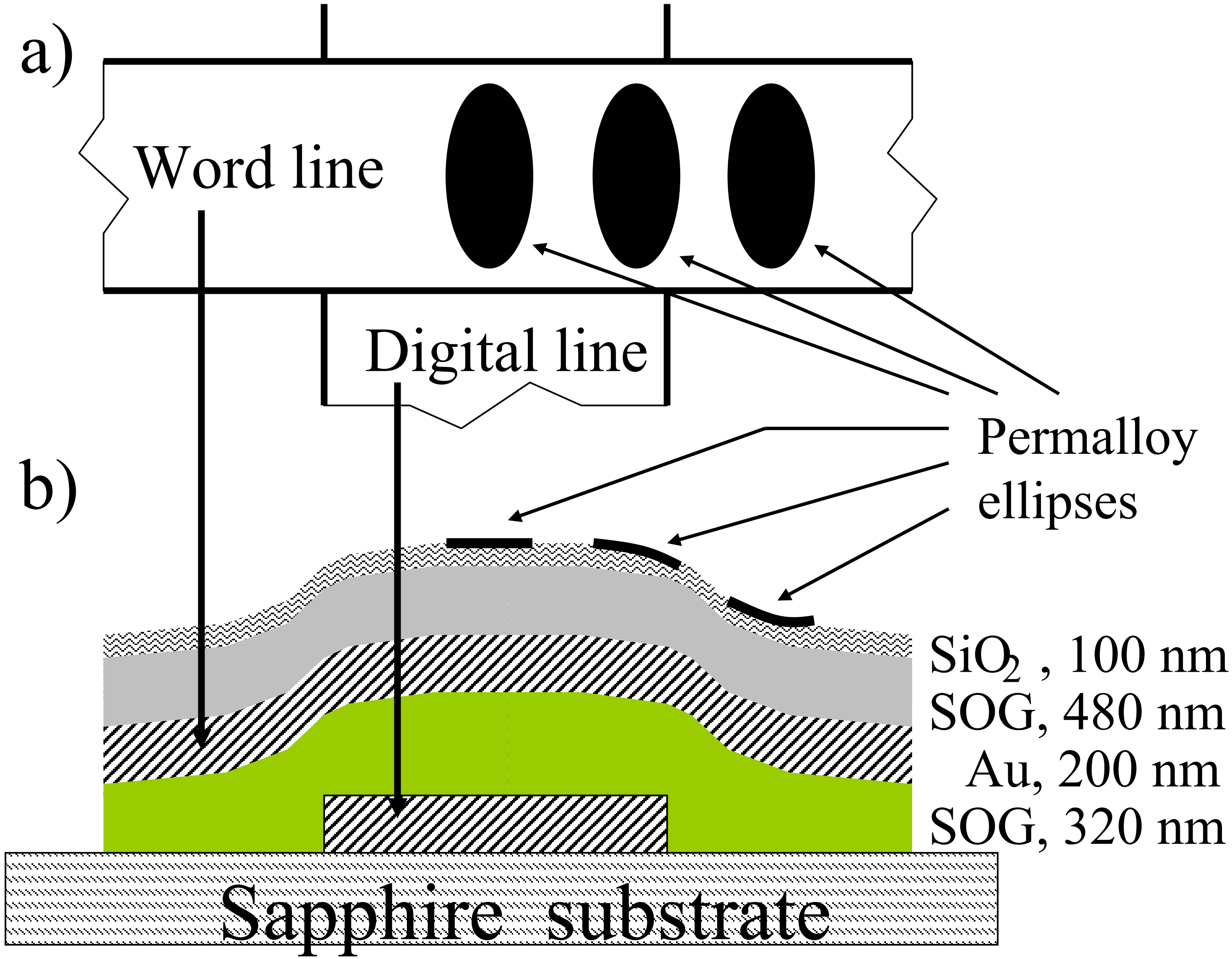

A. Krichevsky

example of switching scenario in “half-select” regime

3x1 μm ellipses;
movie duration – 2.6 ns.

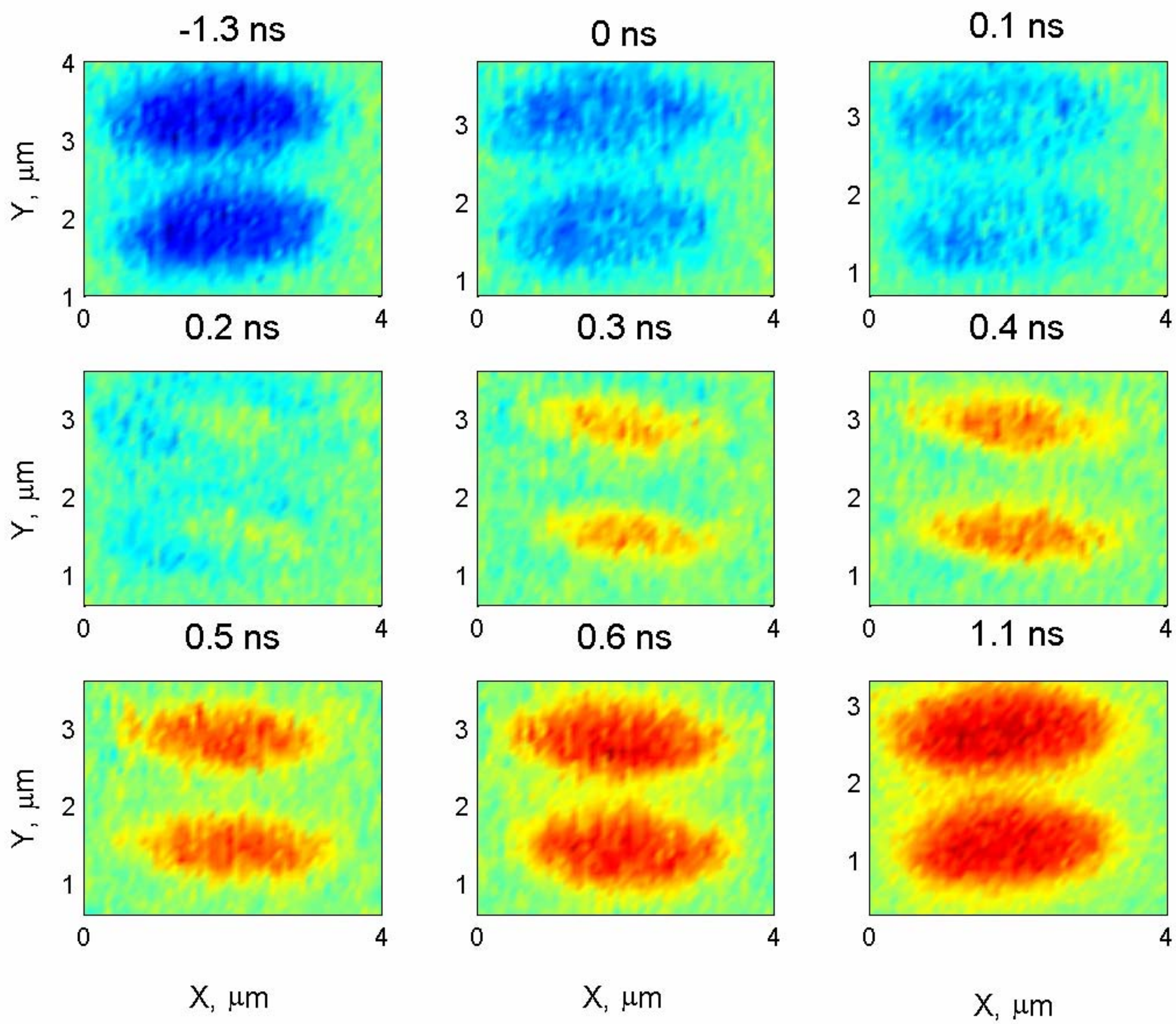

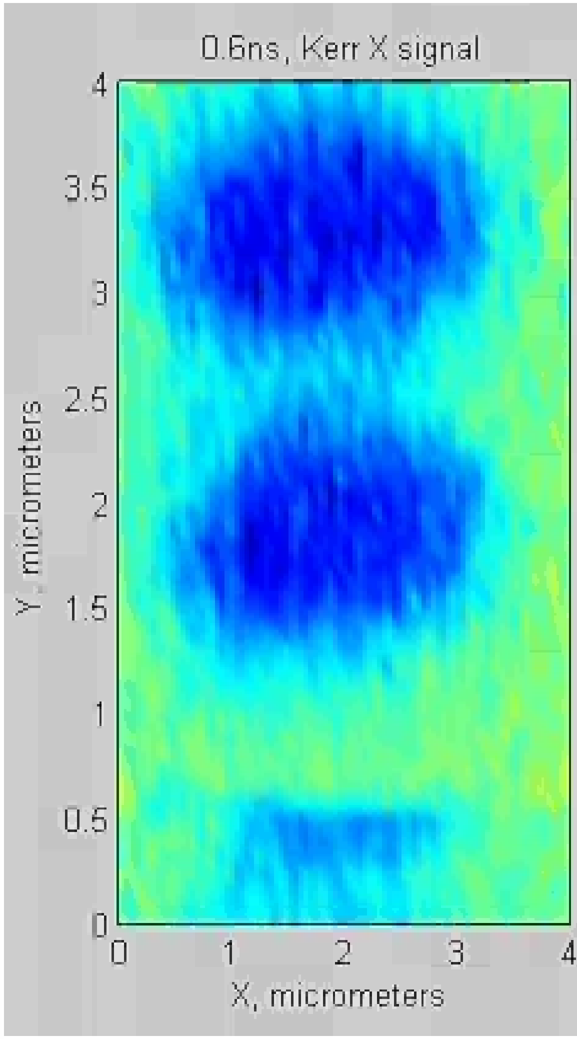

“half-select” switching: simultaneous action of easy- and hard-axis fields required to flip

Stoner-Wolfarth astroid

Energy expression for uniaxial anisotropy:

$$E = K\sin^2\theta - H\mu\cos(\varphi-\theta)$$

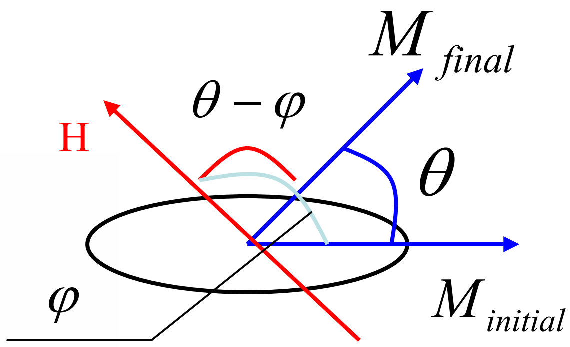

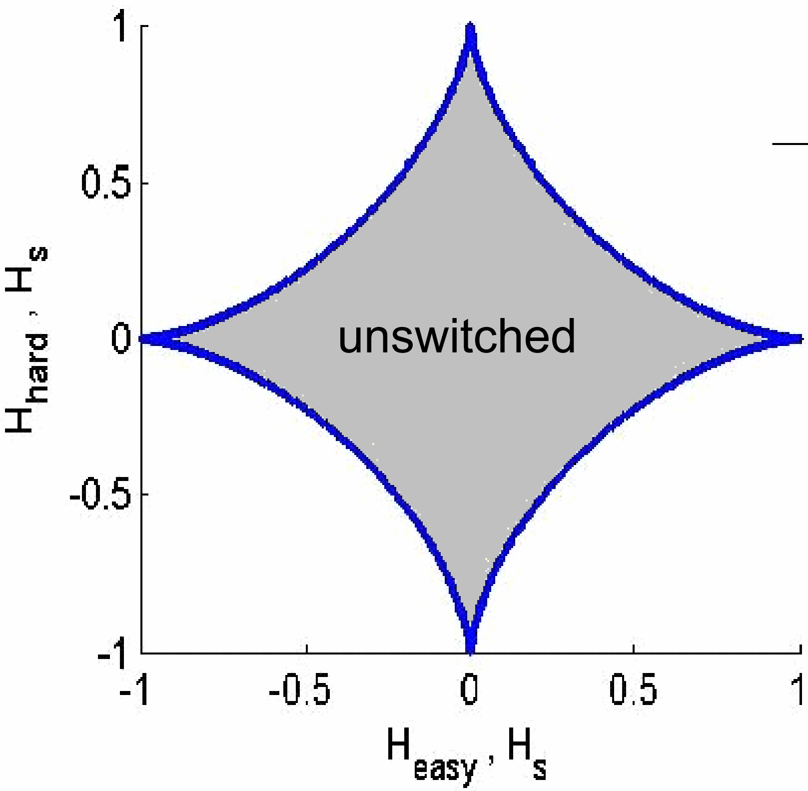

$$\boxed{H_x^{2/3} + H_y^{2/3} = H_{coercivity}^{2/3}}$$

Switching diagram, easy-axis pulse width 0.5 ns

Final state magnetization is measured 20 ns after the pulses end.

Half – select switching at higher easy-axis field (>50 Oe), incomplete switching at lower values.

Pulse timing:

Auxiliary pulse, risetime 250 ps

Principal pulse, risetime 300 ps

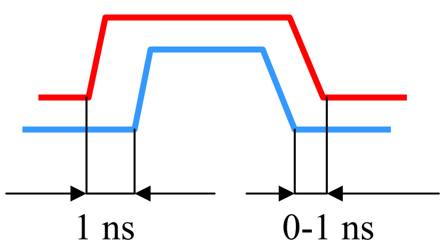

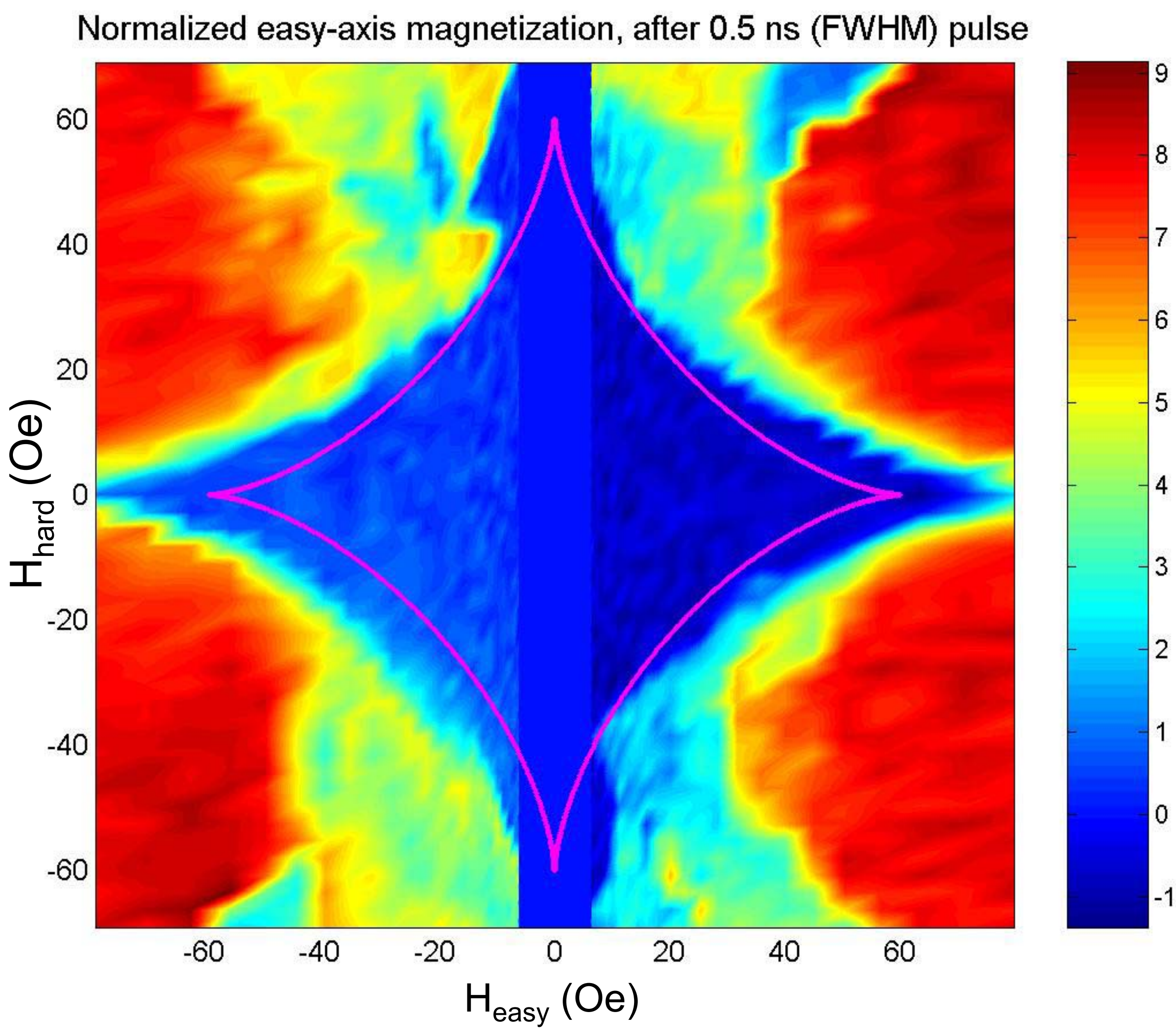

study as a function of pulse durations

switching diagrams rendered according to final magnetization state

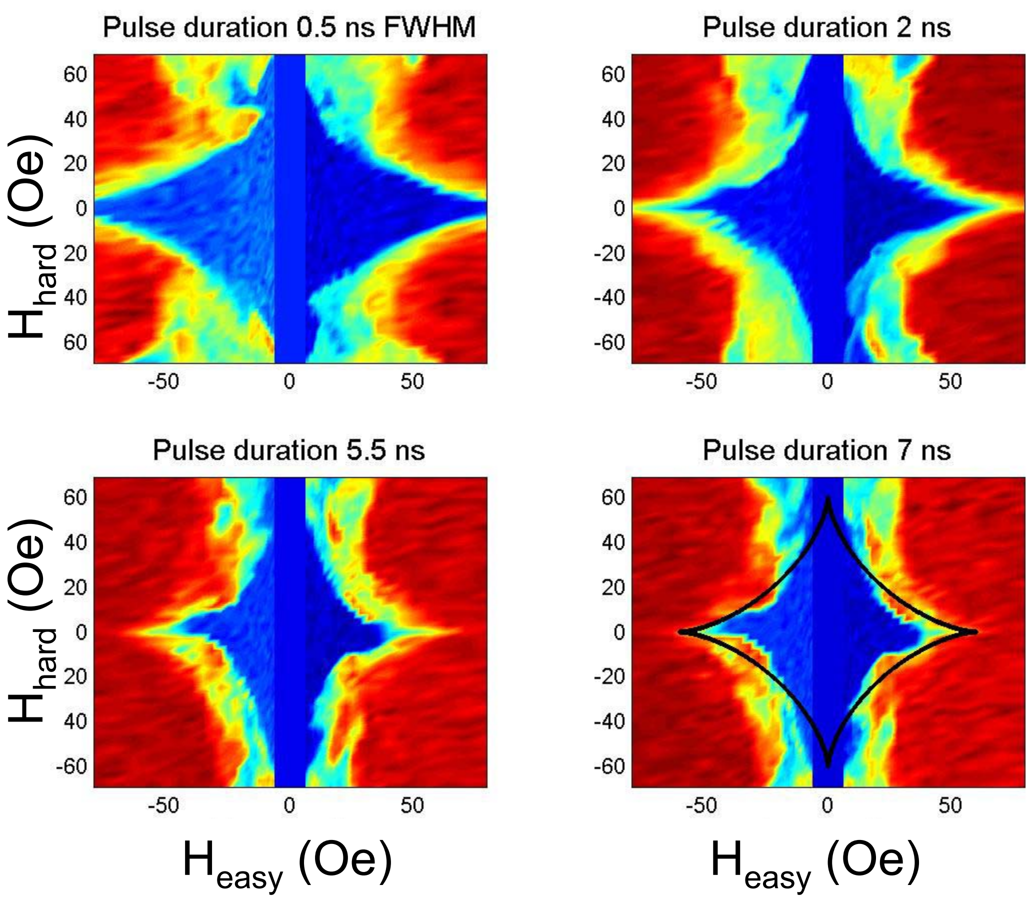

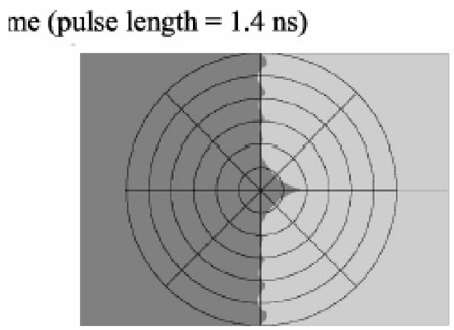

dynamic switching, final states

M. Bauer, J. Fassbender, B. Hillebrands, and R. L. Stamps, “Switching behaviour of a Stoner particle beyond the relaxation time limit,” Phys. Rev. B **61** (5), 3410-3416 (2000)

- switching astroids shrink in the easy axis direction as the pulses duration increase.
- incomplete switching is observed at low easy-axis field values.
- astroids are extended in hard axis direction.
- short pulses (of 0.5 ns FWHM) are sufficient to achieve reliable half-select switching, and their shape doesn’t change significantly at pulse durations of more than 5 ns.
- “pockets” of switching are observed at long pulse durations

“incomplete switching”

basic mechanism = vortex formation

A single vortex often is formed in the case of a weak easy-axis field. Stronger easy-axis field prevents this.

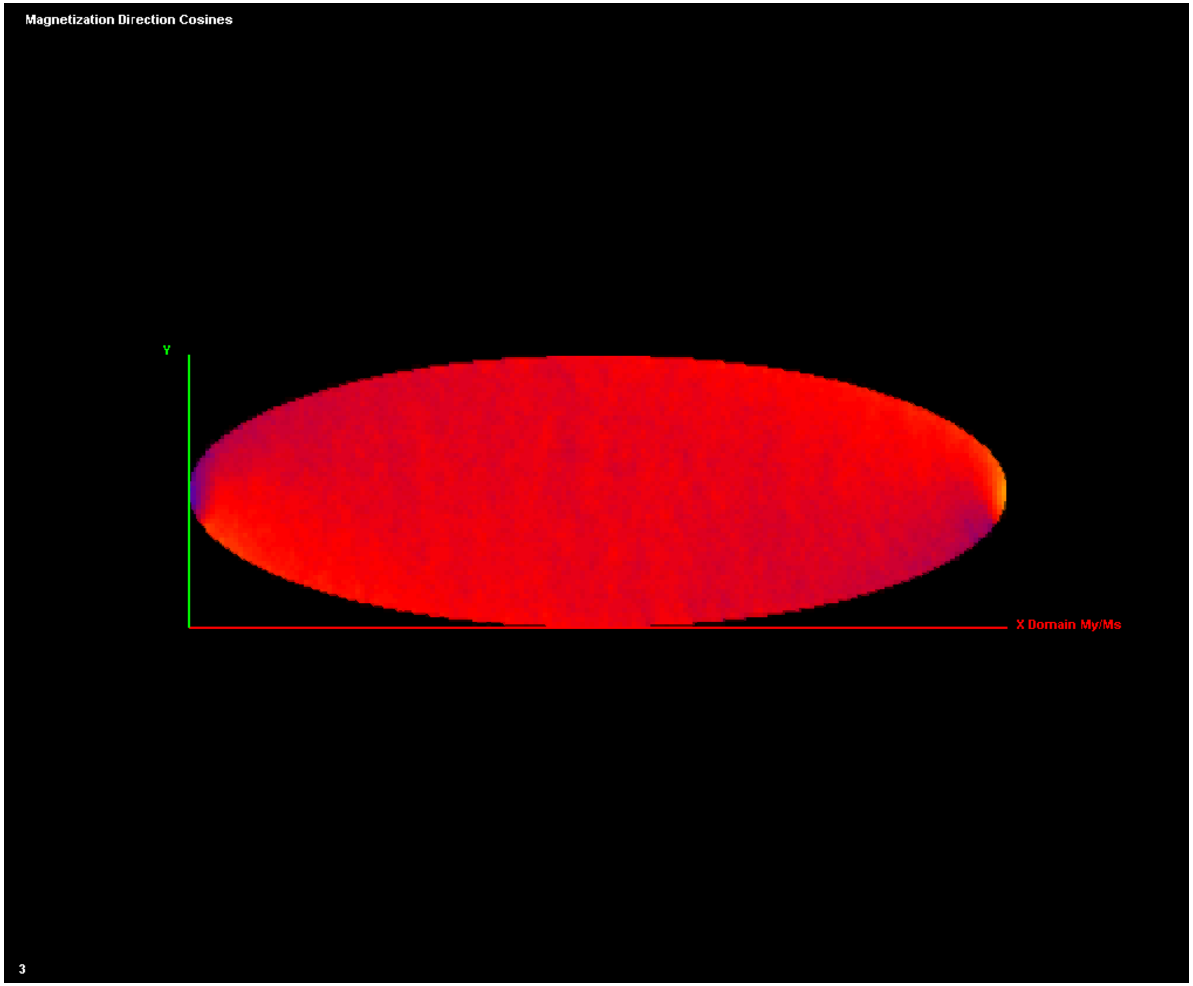

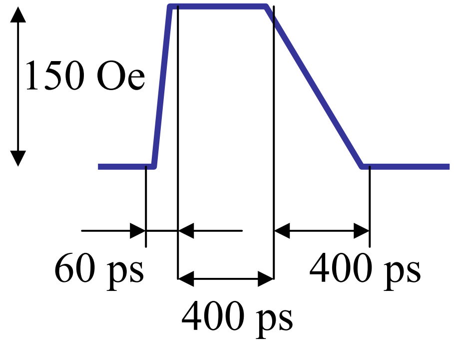

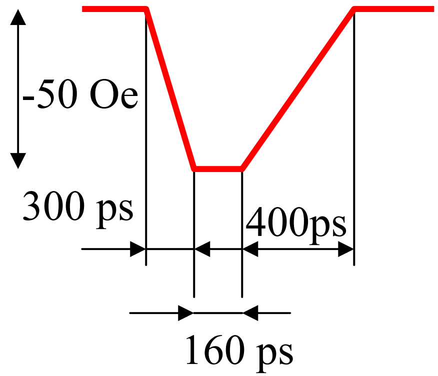

Red = Right
blUe = Up
yellOW = dOWn
grEen = lEft.

“coherent half-select switching”

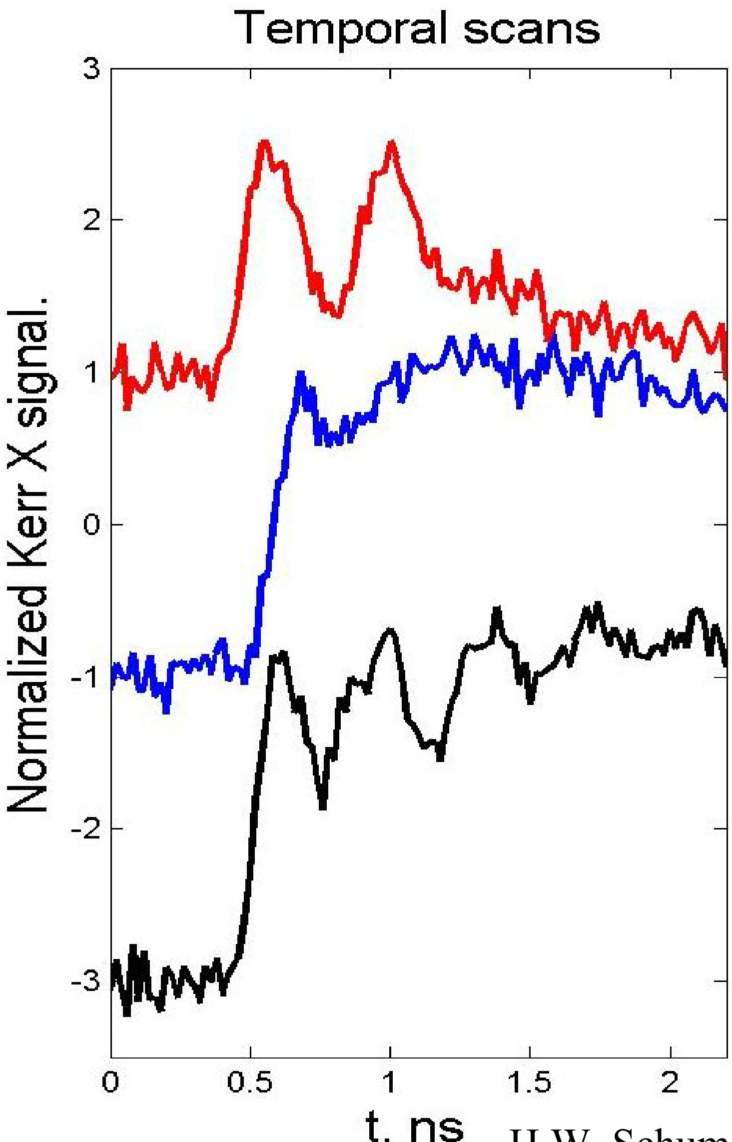

temporal trace for 220 Oe hard axis field only; unswitched at the end.

hard axis pulse assisted by 45 Oe easy-axis field of duration of 0.5 ns Fast switching is achieved, with little ringing.

easy axis pulse delayed ~170 ps with respect to the hard-axis pulse. Different phase at end of pulse yields ringing.

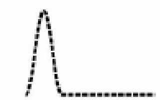

(pulse length = 0.25 ns)

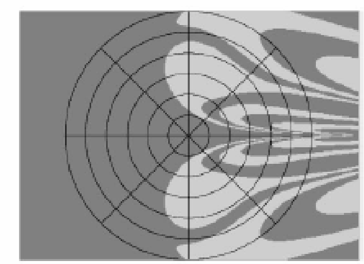

Bauer diagram for SW particle in precessional regime

other related work:

H.W. Schumacher et. al., Phys. Rev. Lett. **90** (1) 2003 017204-1 – 017204-4

Th. Gerrits. et. al., Nature **418**, 509 (2002).

S. Kaka and S.E. Russek, Appl. Phys. Lett. **80**, Feb. 2002.

W.K. Hiebert et. al., J. Appl. Phys. **93**, May 2003.

precessional reversal with fast pulses

experiment vs. simulation, $H_y = 140$ Oe

Both experimental data and simulated evolution of the magnetization demonstrate similar behavior (spiraling in XZ plane) during the coherent phase of switching.

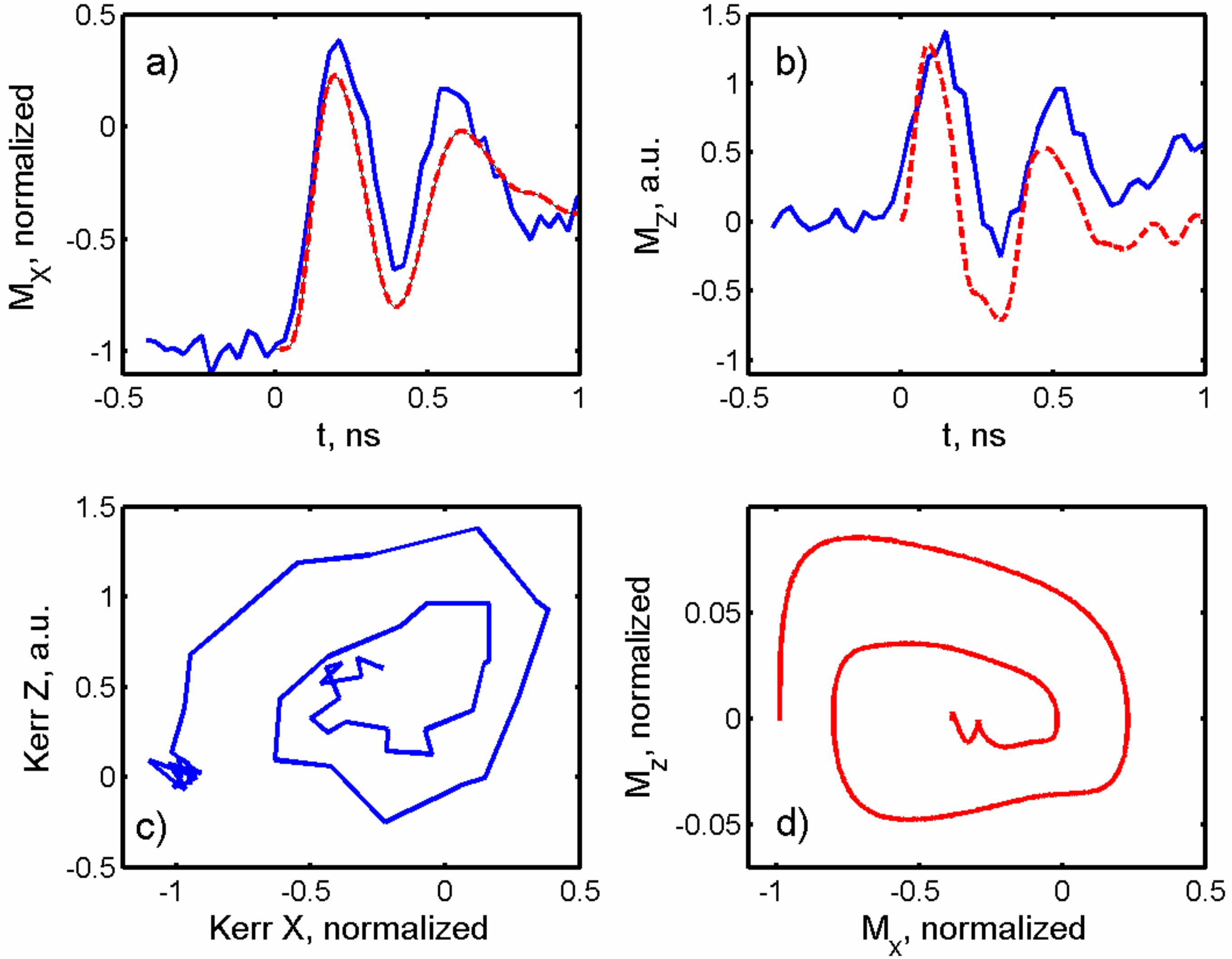

A. Krichevsky and M.R. Freeman, JAP **95** (2004): 6601

Iron Nanocrystals in SiO_2

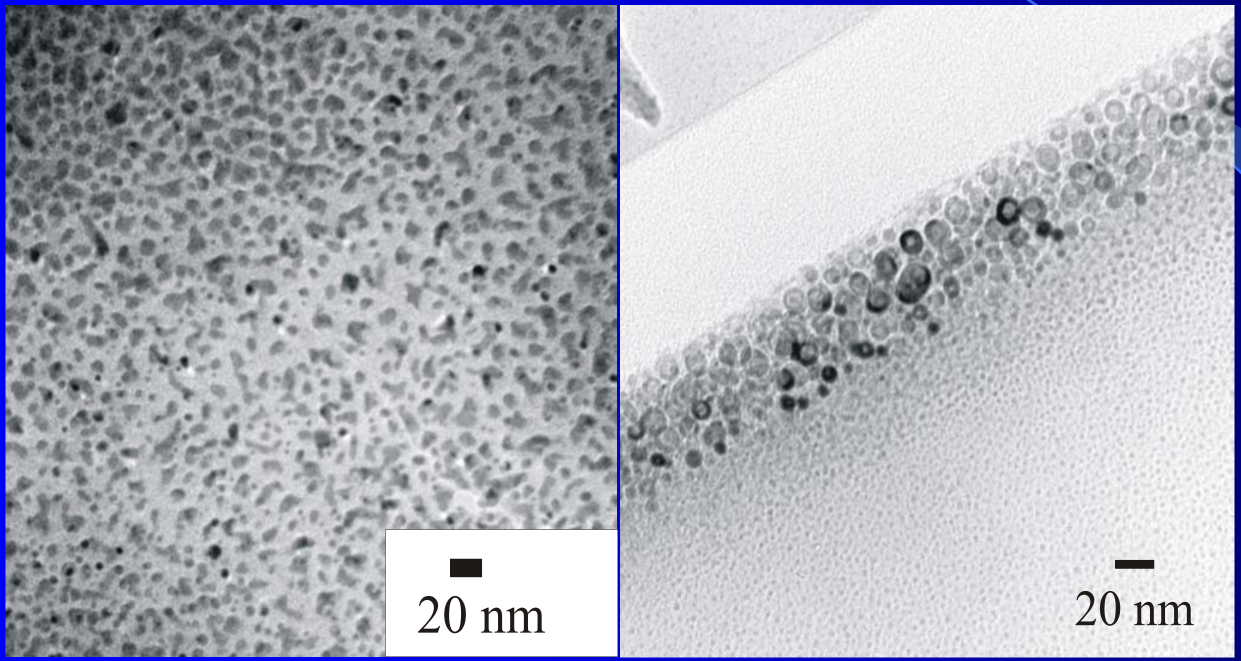

- Fe ions, 80 keV, 1.5×10^{17} ions/cm^2
- Amorphous, high purity SiO_2 host
- As implanted

Ion Implantation:
C.W. White, ORNL

K. Buchanan, A. Meldrum

Iron Implanted (SiO2)

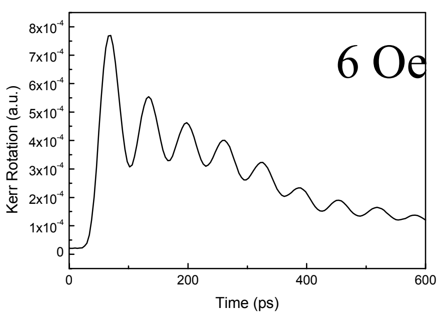

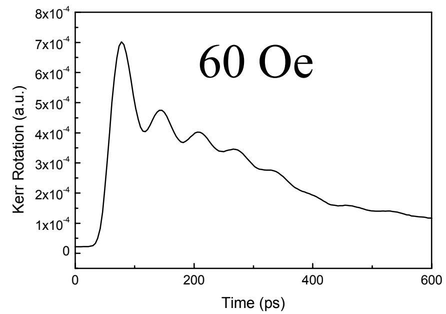

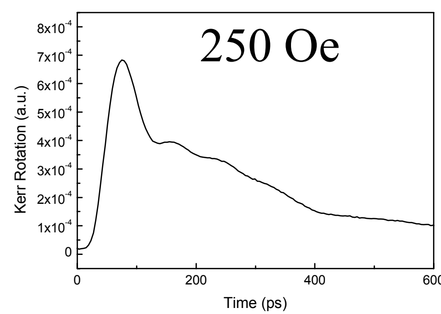

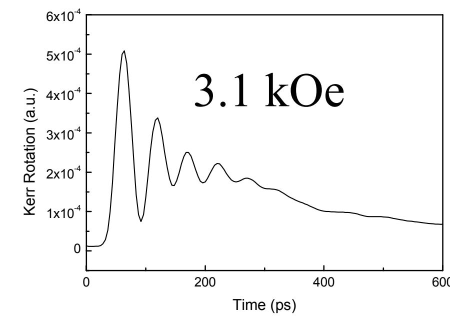

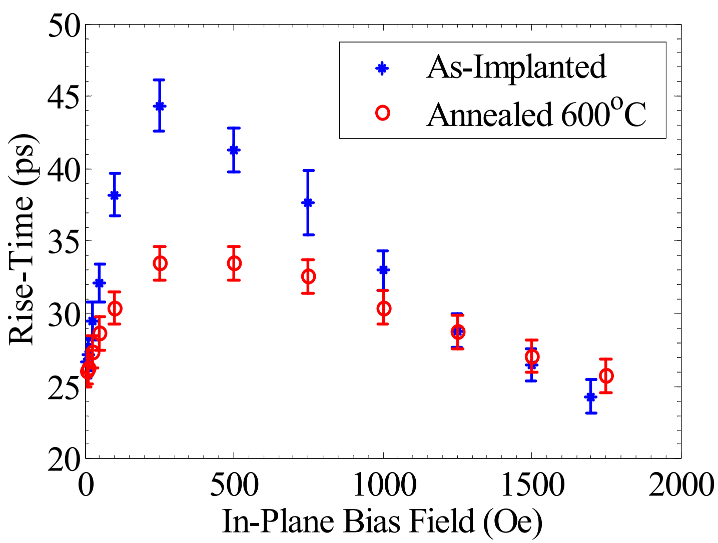

Coupling Induced high frequency precession at zero bias

Nonmonotonic change of precessional frequency (inverse rise time) via external bias field

- Zero-field and high-field rise-times fastest
- Mid-field rise-time slowest
  - Slower for as-implanted sample

Experiment & Simulation

Random

Array

10 nm cubes

2.5 nm cell size

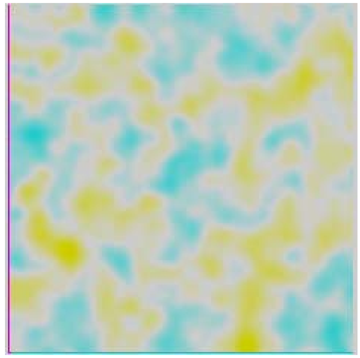

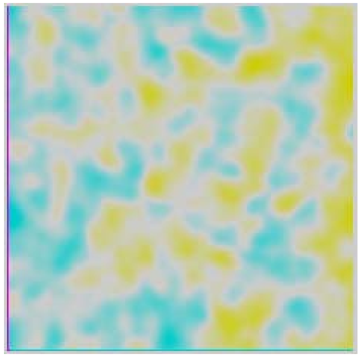

100 Oe

H_z 25 nm above (simulation)

MFM imaging

200 nm

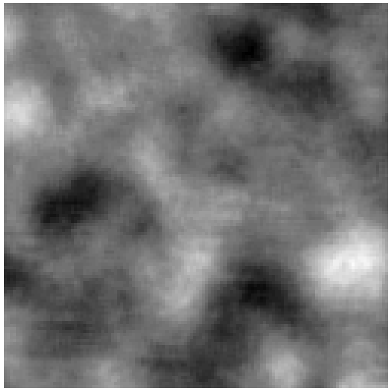

Remanence

Scan Direction

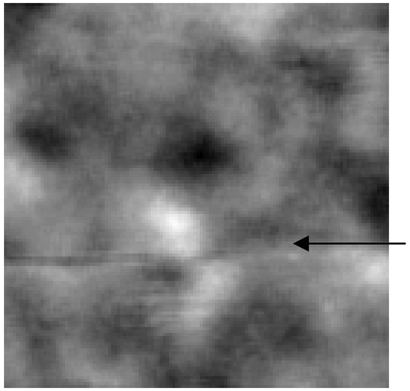

H

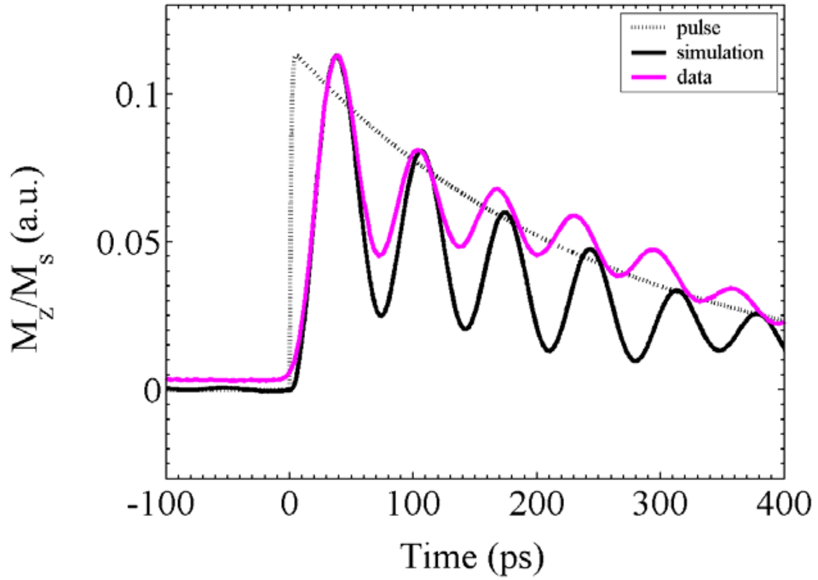

(ii): nanocomposites created via pyrolysis of organometallic polymer precursor

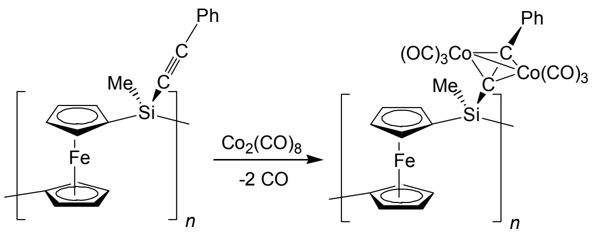

Scheme 1

cobalt-clusterized polyferrocenylsilane (Co-PFS)

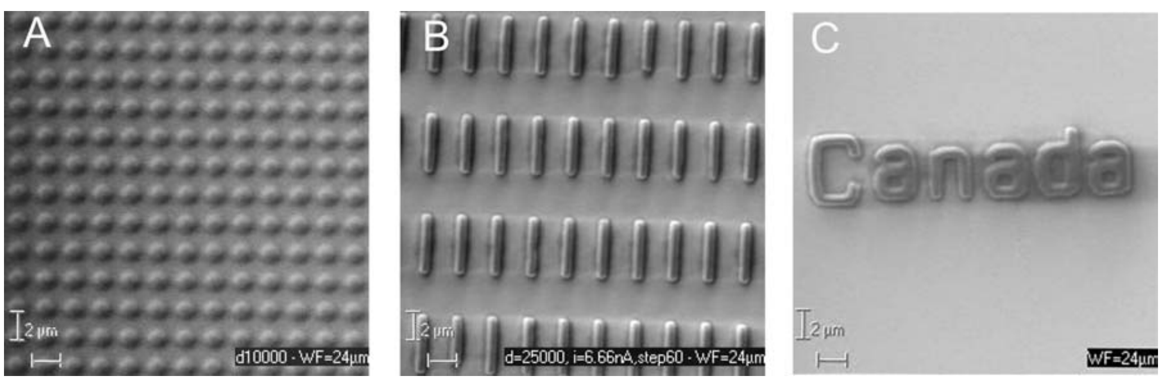

Fig. 1. SEM images of A) dots, B) bars and C) curved lines fashioned by EBL using a Co-PFS resist.

Scott Clendenning, Ian Manners, Univ. of Toronto

Summary

Continuous Film

↓

Magnetic Microstructures

↓

Magnetic Nanostructures

- Uniform excitation, control of damping parameter, dynamic coupling (multilayers)
- Non-uniform magnetization & Pattern Formation
- Complex, ultrafast response, coupling

prospects

- a grand challenge: 3D spatial imaging. behaviour only uniform through the thickness for quasi-2D samples; many other problems associated with fully exploiting the third dimension, but clearing away one major obstacle would have a big impact.
- devil's advocate question (long-term): synchrotron source vs. ultrafast laser-based x-ray source?